Single photon flux imaging with sub-pixel resolution by motion compensation

Martin Laurenzis, Emmanuel Bacher, Trevor Seets, Atul Ingle, Andreas Velten, et al.

Martin Laurenzis, Emmanuel Bacher, Trevor Seets, Atul Ingle, Andreas Velten, Frank Christnacher, "Single photon flux imaging with sub-pixel resolution by motion compensation," Proc. SPIE 12512, Advanced Photon Counting Techniques XVII, 125120E (15 June 2023); doi: 10.1117/12.2663029

Event: SPIE Defense + Commercial Sensing, 2023, Orlando, Florida, United States

Single photon flux imaging with sub-pixel resolution by motion compensation

Martin Laurenzis[a], Emmanuel Bacher[a], Trevor Seets[b], Atul Ingle[c], Andreas Velten[b,d], and Frank Christnacher[a]

[a]French-German Research Institute of Saint-Louis, 5 Rue du General Cassagnou, 68301 Saint-Louis, France
[b]Department of Electrical and Computer Engineering, University of Wisconsin-Madison, Madison, WI 53706, USA
[c]Department of Computer Science, Portland State University, Portland, OR 97201, USA
[d]Department of Biostatistics and Medical Informatics , University of Wisconsin-Madison, Madison, WI 53706, USA

ABSTRACT

Single photon counting avalanche diodes (SPADs) are versatile sensors for active and time-correlated measurements such as ranging and fluorescence imaging. These detectors also have great potential for passive or uncorrelated imaging. Recently, it was demonstrated that passive imaging of photon flux is possible by determining the mean photon arrival time. For ambient light illumination, timestamp data can be interpreted as a metric for the photon impingement rate. Various applications have been investigated including high-dynamic-range imaging, single-photon imaging, and capture of fast-moving objects or dynamic scenes. However, the appearance of noise and motion blur requires sophisticated signal processing that enables sub-pixel resolution imaging and reconstruction of the scene by motion compensation. In this paper, we present new results on the evaluation of global scene motion. In our approach, motion is intentionally generated by a rotating wedge prism, resulting in continuous global motion on a circular path. We have studied scenes with different optical contrast.

Keywords: Single photon counting, uncorrelated sensing, photon flux imaging, motion compensation

1. INTRODUCTION

Due to their ability to precisely measure the time of arrival of individual photons, single photon-counting avalanche diode (SPAD) sensors are gaining popularity for use in various optronic sensing applications in recent years. SPAD sensors can be integrated and manufactured inexpensively in standardized semiconductor manufacturing processes with a wide range of pixel array sizes, from single pixel detectors to megapixel SPAD arrays.[1–6] SPAD sensors have an outstanding sensitivity, low dark count rates and high time resolution of a few picoseconds.

Typically, SPAD sensors are used in conjunction with an active light source (e.g. a pulsed laser) to record the photon timestamps in synchronization with the pulsed illumination source such as in fluorescence lifetime microscopy,[7] range imaging,[8–11] super-resolution ranging,[12] transient[13,14] and non-line-of-sight sensing.[15–18]

Recent publications focused on the passive sensing capabilities of single photon counting devices by, for instance, restoring intensity images from binary photon detection[19–24] for both static and dynamic scenes. Furthermore, the timing ability of SPAD sensors was used to determine the physical intensity by estimation of the photon flux from the photon impingement rate.[25–30] In this approach, the time between photon events is determined from the mean event time. It was shown that with photon flux measurements SPAD sensors are able to perform sensing with high dynamic range.

Further author information: (Send correspondence to M.L.)
E-mail: martin.laurenzis@isl.eu

Advanced Photon Counting Techniques XVII, edited by Mark A. Itzler, Joshua C. Bienfang, K. Alex McIntosh, Proc. of SPIE Vol. 12512, 125120E · © 2023 SPIE · 0277-786X · doi: 10.1117/12.2663029

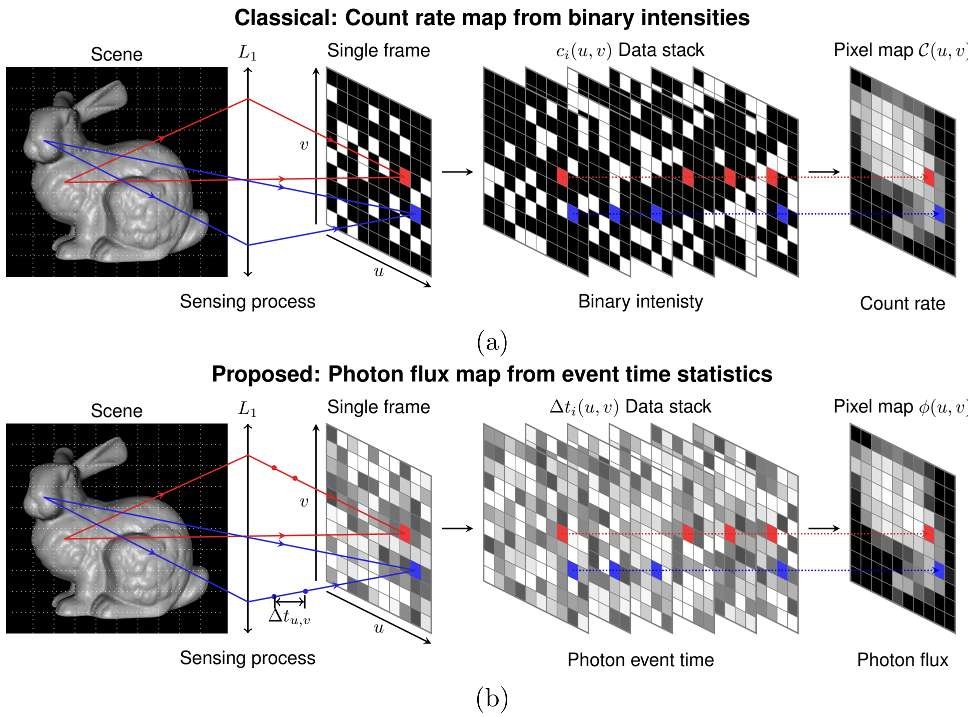

Figure 1. The intensity of the photon flux impinging the SPAD detector is often estimated from (a) the count rate $\mathcal{C}(u, v)$ by analyzing binary intensities that is the counting of photon events, only. In contrast, we analyze (b) the statistical behavior of the photon event time to obtain the photon flux $\phi(u, v)$.

In prior work, we have demonstrated[27] the compensation of motion by accumulating photon information along motion trajectories in these 3D (spatio-temporal) photon timestamp data sets. Further, we have published some investigations on the application of deep neutral network (DNN) image up-scaling.[29,30]

In the current paper, we use a rotating wedge prism (RWP) in the sensor's field of view to intentionally introduce a moving shift of the scene within the image. We use this motion to apply our aforementioned motion compensation algorithm to reduce noise and motion blur, and to increase the resolution within the observed scene.

2. RELATED WORK

Passive Single-Photon Imaging: The passive single-photon imaging aspect is related to work discussing quanta image sensors (QIS),[20–23] binary single photon intensities,[24,31] low noise sCMOS[32] and EMCCD[33] cameras with low light sensitivity. We consider SPAD based imaging here because they provide much higher time resolution compared to these other sensor technologies. Moreover, SPADs can be manufactured cheaply as they are compatible with the CMOS photolithography processes.

Motion De-blurring: Motion de-blurring is an ill-posed inverse problem. Conventional de-blurring techniques pose this as a de-convolution problem, where the blur kernel may be assumed to be known or can be estimated from the image itself .[34,35] Recent methods also use data driven approaches[36] to handle the ill-posed situation

The idea closest related to our work is burst photography where a rapid sequence of images (usually around 10) are captured and merged after motion compensation.[23] Our method takes this idea to the extreme limit where the burst is composed of single-photon frames.[22,28]

Super-resolution and binary Image Up-sampling: The task of image up-scaling is a well studied problem. Many methods use a sub-pixel movement through deliberate changes in the position of the image plane[37–40] or analyze in-scene motion[41,42] for resolution enhancement through analysis of image sequences. For single image processing, state-of-the-art methods apply data-driven approaches to train and employ deep neural networks[43] to obtain super-resolution images from low resolution data-sets. Several studies were published refining, using and comparing different approaches.[44–51] Here we leverage these developments and apply them to the new kind of data provided by a single-photon camera.

3. PASSIVE PHOTON TIMING

In principle there are two approaches to derive information about the amount of light impinging a single photon counting detector, as depicted in Fig. 1. First, (a) we can determine the intensity as a count rate from binary samples and second (b), we estimate the photon flux from the photon timing data.

In the first case, the count rate from binary samples approach, we simply count the number of photon events N_τ within a certain time span τ e.g. exposure time. The count rate c_τ is the quotient of both, see Eq. 1. Some groups are working on methods to estimate the intensity from a only few samples.[19,24]

$$c_\tau = \frac{N_\tau}{\tau} \tag{1}$$

We proposed a second approach based on analyzing to timing behavior of passive photons or ambient light. Generally speaking, we try to estimate the mean waiting time $\bar{t}$ between two photon events to derive the photon flux $\hat{\phi}$ as the inverse waiting time, see Eq. 2. We assume that we have a limited number of samples m and will detect $n \ll m$ photons. Further, $\hat{\phi}$ is an estimator which comply with the Poisson statistics.

$$\hat{\phi} = \frac{1}{\bar{t}}, \text{ with } \bar{t} = \sum_{j=1}^{m} \frac{t_j}{n_j} = \frac{\sum_{j=1}^{m} t_j}{n} \tag{2}$$

In previous work,[25–30] we have shown that, in principle, we can reduce the number of detected photons to a single photon, $n_{min.} \rightarrow 1$. $\hat{\phi}$ becomes the instantaneous photon flux $\hat{\phi}_{\text{inst.}}$

$$\hat{\phi}_{\textbf{inst.}} = \frac{1}{t_{\textbf{inst.}}}, \textbf{ with } t_{\textbf{inst.}} = \sum_{j=1}^{\mu} t_j \textbf{ and } \sum_{j=1}^{\mu} n_j \equiv 1 \tag{3}$$

4. COMPENSATION OF AN ARBITRARY MOTION

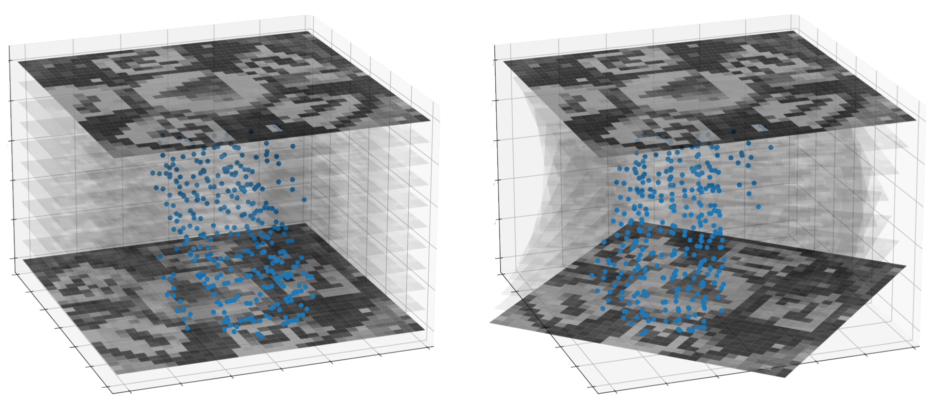

(a) (b)

Figure 2. We have developed an algorithm to calculate the photon flux and blurring due to compensate motion. The data stack (a) is analyzed locating statistical change-points. Each frame of the data stack (b) is transformed (rotation, translation) to minimize blurring and to enable the photon flux calculation along the motion trajectories. Using prior up-scaled data frames can enable super-resolution.

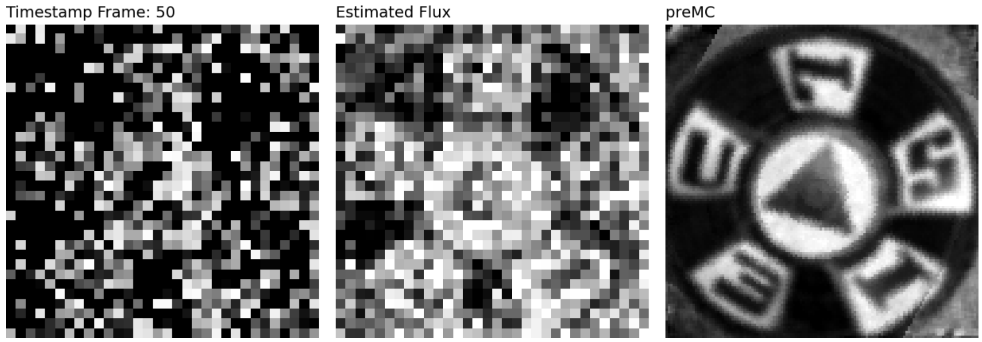

Figure 3. Experimental results imaging a rotating fan (from left to right): a single time stamp frame, the corresponding estimated photon flux at that instant and result of the algorithm (preMC) performing motion compensation of pre-scaled data frames.

It is obvious that the instantaneous photon flux estimation (Eq.3) is prone to noise due to the direct impact of the photon detection statistics. To compensate this effect, we have developed a high performance noise reduction algorithm based on the evaluation of the photon statistics in the whole data set (time series of photon detection frames) and on the analysis of statistical change points. The full algorithm is described in detail elsewhere.[27,30]

In short, we detect statistical change points in the data stack, as illustrated in Fig. 2. These change points are caused by changes in the photon flux due to motion of areas with high optical contrast in the observed scene. In a second step we estimate the transform matrix (e.g. Euclidean transforms) between consecutive data frames and re-orientate the data stack to compensate motion in the scene, as illustrated in Fig. 2 (b). Finally, we can calculate the mean photon flux a long the motion trajectories for every position. Additionally, we have shown that using prior scaled data sets (e.g. scaling from 32×32 to 128×128) we can obtain sub-pixel resolution while reducing significantly the motion blur in the scene.[27,30]

In Figure 3 we show some results obtained with our motion compensation algorithm. On the left, a single frame of our data stack is shown containing timestamp data. In the middle, a fist estimate of the photon flux is presented. This frame illustrates the low resolution (32×32 pixel) image before up-scaling and compensation of motion is applied. The final result is given on the right side. After applying our algorithm, we obtain a high-resolution (128×128 pixel) image in which many details can be seen that were previously not visible due to low resolution and noise. Thanks to the continuous movement in the image and the precise realignment of the image frames, we can detect structures with sub-pixel resolution.

5. COMPENSATION OF AN INTENDED MOTION

Although we have achieved impressive results with our motion compensation algorithm that detects arbitrary motion in the scene, as described above, we run into a few problems. First, we only obtain super-resolution for objects that are constantly moving. Imaging static scenes or non-moving areas of the scene does not benefit from the previously up-scaled resolution and can become blurry. Second, imaging non-monotonic or very dynamic motion (such as an exploding balloon) is also problematic, as our approach works best with Euclidean transformations and motion that persists over many frames.

As illustrated in Fig. 4 (a), we use a single photon counting avalanche diode (SPAD) camera (PF32, PhotonForce, UK) with an array of 32×32 sensors to observe a scene illuminated by an un-correlated light source. Further, to overcome the aforementioned main problems, we have modified our experimental setup with the goal of ensuring constant motion throughout the scene. In detail, we introduced a rotating wedge prism into the sensor's field of view.

This prism (Thorlab, US, PS810-A) deflects the field of view by a few degrees. The prism is installed on a flat frame-less motor (Maxon, CH, EC frame-less 90 flat) which rotates the prism around the optical axis and thus the deflection direction of the field of view. As illustrated in Fig. 4 (d), we can observe a linear displacement

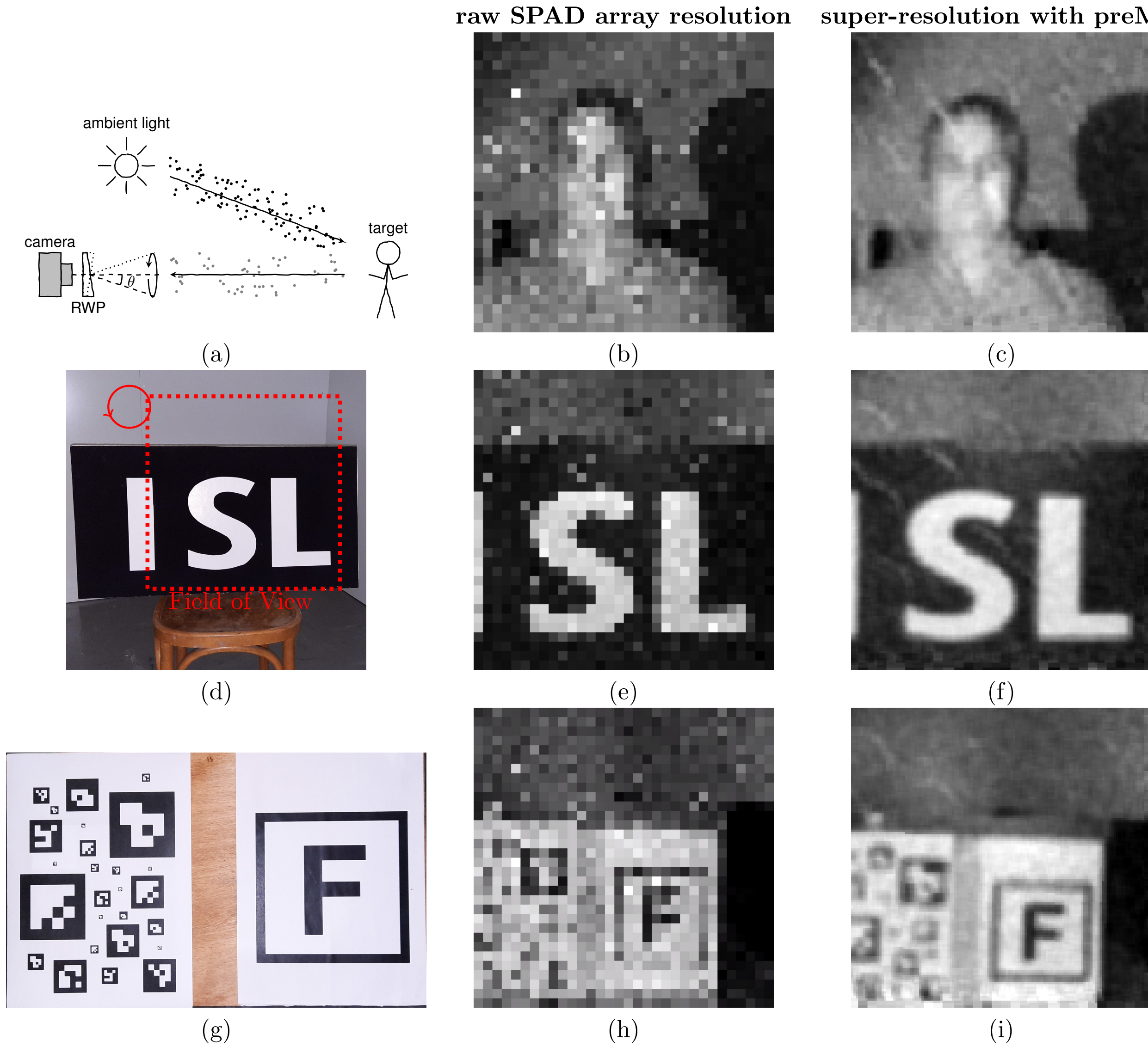

Figure 4. Illustration of the modified setup (a) setup using a SPAD camera with a rotating wedge prism (RWP) to deflect the field of view by an angle θ and experimental results imaging a letter board (upper row) and a person (bottom row). In both cases we show the raw SPAD array resolution and the super-resolution obtained with the preMC algorithm.

of the field of view which moves circularly around a center. In the experiments, we used a rotation speed of 5000 rpm or 83 Hz. In our approach we do not use the rotation state to estimate the motion in the image.

Some first results are shown in Figure 4. First, we imaged the face of a person (one of the authors) sitting in front of the sensor, see Fig. 4 (b) and (c). Although, the optical contrast in this scene is low, we are able to apply the motion compensation algorithm and obtain a significant resolution enhancement. In this enhanced image, we can start to distinguish between different areas of the face and can identify, for instance, nose, mouth, eyes and eyebrows.

In a second experiment, we investigate a "letter" scene (Fig. 4 (d)) with high optical contrast consisting of a black board and randomly selected white letters ("I", "S" and "L"). In the image, we indicate in the sensor's field of view (red dots) and its movement along a circular path (red circle). The fist estimation of the photon flux is shown in (e). Here, we obtain the original low resolution of the camera. Using our motion compensation algorithm with a prior scaled dataset (f), we can reconstruct a super-resolution image of the scene.

Finally, we used a high contrast board (Fig. 4 (g)) with a letter "F" (right) and ArUco-tags[52] with different patterns and sizes (left). Low resolution and super-resolution images are shown in Fig. 4 (h) and (i), respectively.. With our method, we are able to detect structures (frames around "F" and small tags) and read tags whose structures are below the spatial resolution of the sensor.

6. DISCUSSION AND CONCLUSIONS

We have investigated passive single photon timing to estimate the photon flux impinging the sensor. We have introduced the concept of instantaneous photon flux using the timing of a single photon event and explained the motion compensation algorithm using prior scaled imaging. This approach can result in high resolution reconstruction of the photon flux and suppresses statistical noise and motion blur. Further, we have identified two main problems of this approach: we cannot obtain super-resolution in areas without motion and areas with short or non-continuous motion. To overcome these problems, we have modified our setup and introduced a rotating wedge prism into the sensor's field of view to introduce a constant motion of the whole scene.

We have investigated three different scenes and obtained high resolution reconstruction of the photon flux in both scenes. The first scene was a person sitting in front of the camera, second, a "letter" board with very high optical contrast and third, a board with small tags. All scenes represent static or low motion scenarios. Further, in all cases, it was possible to reconstruct an up-scaled image with significantly increased resolution (sub-pixel).

In further research, we need to clarify whether this modified detection approach can also be used to detect non-continuous motion in a scene, such as an exploding balloon, a person waving their hands or persons walking in different directions.

REFERENCES

[1] Charbon, E., "Single-photon imaging in complementary metal oxide semiconductor processes," *Philosophical Transactions of the Royal Society A: Mathematical, Physical and Engineering Sciences* **372**(2012), 20130100 (2014).

[2] Richardson, J., Walker, R., Grant, L., Stoppa, D., Borghetti, F., Charbon, E., Gersbach, M., and Henderson, R. K., "A 32× 32 50ps resolution 10 bit time to digital converter array in 130nm cmos for time correlated imaging," in [*2009 IEEE Custom Integrated Circuits Conference*], 77–80, IEEE (2009).

[3] Veerappan, C., Richardson, J., Walker, R., Li, D.-U., Fishburn, M. W., Maruyama, Y., Stoppa, D., Borghetti, F., Gersbach, M., Henderson, R. K., et al., "A 160× 128 single-photon image sensor with on-pixel 55ps 10b time-to-digital converter," in [*2011 IEEE International Solid-State Circuits Conference*], 312–314, IEEE (2011).

[4] Kumagai, O., Ohmachi, J., Matsumura, M., Yagi, S., Tayu, K., Amagawa, K., Matsukawa, T., Ozawa, O., Hirono, D., Shinozuka, Y., et al., "A 189x600 back-illuminated stacked spad direct time-of-flight depth sensor for automotive lidar systems," in [*2021 IEEE International Solid-State Circuits Conference (ISSCC)*], **64**, 110–112, IEEE (2021).

[5] Villa, F., Lussana, R., Bronzi, D., Tisa, S., Tosi, A., Zappa, F., Dalla Mora, A., Contini, D., Durini, D., Weyers, S., et al., "Cmos imager with 1024 spads and tdcs for single-photon timing and 3-d time-of-flight," *IEEE journal of selected topics in quantum electronics* **20**(6), 364–373 (2014).

[6] Guerrieri, F., Tisa, S., Tosi, A., and Zappa, F., "Two-dimensional spad imaging camera for photon counting," *IEEE Photonics Journal* **2**(5), 759–774 (2010).

[7] Bruschini, C., Homulle, H., Antolovic, I. M., Burri, S., and Charbon, E., "Single-photon avalanche diode imagers in biophotonics: review and outlook," *Light: Science & Applications* **8**(1), 1–28 (2019).

[8] Albota, M. A., Heinrichs, R. M., Kocher, D. G., Fouche, D. G., Player, B. E., O'Brien, M. E., Aull, B. F., Zayhowski, J. J., Mooney, J., Willard, B. C., et al., "Three-dimensional imaging laser radar with a photon-counting avalanche photodiode array and microchip laser," *Applied optics* **41**(36), 7671–7678 (2002).

[9] Kirmani, A., Venkatraman, D., Shin, D., Colaço, A., Wong, F. N., Shapiro, J. H., and Goyal, V. K., "First-photon imaging," *Science* **343**(6166), 58–61 (2014).

[10] Gupta, A., Ingle, A., and Gupta, M., "Asynchronous single-photon 3d imaging," in [*Proceedings of the IEEE/CVF International Conference on Computer Vision*], 7909–7918 (2019).

[11] Tobin, R., Halimi, A., McCarthy, A., Laurenzis, M., Christnacher, F., and Buller, G. S., "Three-dimensional single-photon imaging through obscurants," *Optics express* **27**(4), 4590–4611 (2019).

[12] Tobin, R., Halimi, A., McCarthy, A., Soan, P. J., and Buller, G. S., "Robust real-time 3d imaging of moving scenes through atmospheric obscurant using single-photon lidar," *Scientific Reports* **11**(1), 1–13 (2021).

[13] O'Toole, M., Heide, F., Lindell, D. B., Zang, K., Diamond, S., and Wetzstein, G., "Reconstructing transient images from single-photon sensors," in [*Proceedings of the IEEE Conference on Computer Vision and Pattern Recognition*], 1539–1547 (2017).

[14] Sun, Q., Dun, X., Peng, Y., and Heidrich, W., "Depth and transient imaging with compressive spad array cameras," in [*Proceedings of the IEEE Conference on Computer Vision and Pattern Recognition*], 273–282 (2018).

[15] Kirmani, A., Hutchison, T., Davis, J., and Raskar, R., "Looking around the corner using transient imaging," in [*2009 IEEE 12th International Conference on Computer Vision*], 159–166, IEEE (2009).

[16] Buttafava, M., Zeman, J., Tosi, A., Eliceiri, K., and Velten, A., "Non-line-of-sight imaging using a time-gated single photon avalanche diode," *Optics express* **23**(16), 20997–21011 (2015).

[17] Faccio, D., Velten, A., and Wetzstein, G., "Non-line-of-sight imaging," *Nature Reviews Physics* **2**(6), 318–327 (2020).

[18] Laurenzis, M., Klein, J., Bacher, E., and Metzger, N., "Multiple-return single-photon counting of light in flight and sensing of non-line-of-sight objects at shortwave infrared wavelengths," *Optics letters* **40**(20), 4815–4818 (2015).

[19] Altmann, Y., Aspden, R., Padgett, M., and McLaughlin, S., "A bayesian approach to denoising of single-photon binary images," *IEEE Transactions on Computational Imaging* **3**(3), 460–471 (2017).

[20] Fossum, E. R., "The quanta image sensor (qis): concepts and challenges," in [*Imaging Systems and Applications*], JTuE1, Optical Society of America (2011).

[21] Fossum, E. R., "Modeling the performance of single-bit and multi-bit quanta image sensors," *IEEE Journal of the Electron Devices Society* **1**(9), 166–174 (2013).

[22] Chi, Y., Gnanasambandam, A., Koltun, V., and Chan, S. H., "Dynamic low-light imaging with quanta image sensors," in [*European conference on computer vision*], 122–138, Springer (2020).

[23] Ma, S., Gupta, S., Ulku, A. C., Bruschini, C., Charbon, E., and Gupta, M., "Quanta burst photography," *ACM Transactions on Graphics (TOG)* **39**(4), 79–1 (2020).

[24] Yang, F., Lu, Y. M., Sbaiz, L., and Vetterli, M., "Bits from photons: Oversampled image acquisition using binary poisson statistics," *IEEE Transactions on image processing* **21**(4), 1421–1436 (2011).

[25] Ingle, A., Velten, A., and Gupta, M., "High flux passive imaging with single-photon sensors," in [*Proceedings of the IEEE/CVF Conference on Computer Vision and Pattern Recognition*], 6760–6769 (2019).

[26] Laurenzis, M., "Single photon range, intensity and photon flux imaging with kilohertz frame rate and high dynamic range," *Optics express* **27**(26), 38391–38403 (2019).

[27] Seets, T., Ingle, A., Laurenzis, M., and Velten, A., "Motion adaptive deblurring with single-photon cameras," in [*Proceedings of the IEEE/CVF Winter Conference on Applications of Computer Vision*], 1945–1954 (2021).

[28] Ingle, A., Seets, T., Buttafava, M., Gupta, S., Tosi, A., Gupta, M., and Velten, A., "Passive inter-photon imaging," *arXiv preprint arXiv:2104.00059* (2021).

[29] Laurenzis, M., Seets, T., Bacher, E., Ingle, A., and Velten, A., "Passive imaging of single photon flux: strategies for de-noising, motion blur reduction and super-resolution up-scaling," in [*Emerging Imaging and Sensing Technologies for Security and Defence VI*], **11868**, 9–15, SPIE (2021).

[30] Laurenzis, M., Seets, T., Bacher, E., Ingle, A., and Velten, A., "Comparison of super-resolution and noise reduction for passive single-photon imaging," *Journal of Electronic Imaging* **31**(3), 033042–033042 (2022).

[31] Carrara, L., Niclass, C., Scheidegger, N., Shea, H., and Charbon, E., "A gamma, x-ray and high energy proton radiation-tolerant cis for space applications," in [*2009 IEEE International Solid-State Circuits Conference-Digest of Technical Papers*], 40–41, IEEE (2009).

[32] Kobayashi, M., Onuki, Y., Kawabata, K., Sekine, H., Tsuboi, T., Muto, T., Akiyama, T., Matsuno, Y., Takahashi, H., Koizumi, T., et al., "A $1.8e^{-}_{rms}$ temporal noise over 110-db-dynamic range 3.4 μm pixel pitch global-shutter CMOS image sensor with dual-gain amplifiers SS-ADC, light guide structure, and multiple-accumulation shutter," *IEEE Journal of Solid-State Circuits* **53**(1), 219–228 (2017).

[33] Daigle, O., Carignan, C., Gach, J.-L., Guillaume, C., Lessard, S., Fortin, C.-A., and Blais-Ouellette, S., "Extreme faint flux imaging with an emccd," *Publications of the Astronomical Society of the Pacific* **121**(882), 866 (2009).

[34] Xu, L. and Jia, J., "Two-phase kernel estimation for robust motion deblurring," in [*European conference on computer vision*], 157–170, Springer (2010).

[35] Pan, J., Liu, R., Su, Z., and Gu, X., "Kernel estimation from salient structure for robust motion deblurring," *Signal Processing: Image Communication* **28**(9), 1156–1170 (2013).

[36] Chakrabarti, A., "A neural approach to blind motion deblurring," in [*European conference on computer vision*], 221–235, Springer (2016).

[37] Kim, S., Bose, N. K., and Valenzuela, H. M., "Recursive reconstruction of high resolution image from noisy undersampled multiframes," *IEEE Transactions on Acoustics, Speech, and Signal Processing* **38**(6), 1013–1027 (1990).

[38] Park, S. C., Park, M. K., and Kang, M. G., "Super-resolution image reconstruction: a technical overview," *IEEE signal processing magazine* **20**(3), 21–36 (2003).

[39] Ben-Ezra, M., Zomet, A., and Nayar, S. K., "Jitter camera: High resolution video from a low resolution detector," in [*Proceedings of the 2004 IEEE Computer Society Conference on Computer Vision and Pattern Recognition, 2004. CVPR 2004.*], **2**, II–II, IEEE (2004).

[40] Ben-Ezra, M., Zomet, A., and Nayar, S. K., "Video super-resolution using controlled subpixel detector shifts," *IEEE transactions on pattern analysis and machine intelligence* **27**(6), 977–987 (2005).

[41] Bascle, B., Blake, A., and Zisserman, A., "Motion deblurring and super-resolution from an image sequence," in [*European conference on computer vision*], 571–582, Springer (1996).

[42] Nayar, S. K. and Ben-Ezra, M., "Motion-based motion deblurring," *IEEE transactions on pattern analysis and machine intelligence* **26**(6), 689–698 (2004).

[43] Dong, C., Loy, C. C., He, K., and Tang, X., "Image super-resolution using deep convolutional networks," *IEEE Transactions on Pattern Analysis and Machine Intelligence* **38**(2), 295–307 (2016).

[44] Dong, C., Loy, C. C., and Tang, X., "Accelerating the super-resolution convolutional neural network," in [*Computer Vision – ECCV 2016*], Leibe, B., Matas, J., Sebe, N., and Welling, M., eds., 391–407, Springer International Publishing, Cham (2016).

[45] Lai, W.-S., Huang, J.-B., Ahuja, N., and Yang, M.-H., "Fast and accurate image super-resolution with deep laplacian pyramid networks," *IEEE Transactions on Pattern Analysis and Machine Intelligence* **41**(11), 2599–2613 (2019).

[46] Zhang, Y., Tian, Y., Kong, Y., Zhong, B., and Fu, Y., "Residual dense network for image super-resolution," in [*Proceedings of the IEEE Conference on Computer Vision and Pattern Recognition (CVPR)*], (June 2018).

[47] Ledig, C., Theis, L., Huszar, F., Caballero, J., Cunningham, A., Acosta, A., Aitken, A., Tejani, A., Totz, J., Wang, Z., and Shi, W., "Photo-realistic single image super-resolution using a generative adversarial network," in [*Proceedings of the IEEE Conference on Computer Vision and Pattern Recognition (CVPR)*], (July 2017).

[48] Wang, X., Yu, K., Wu, S., Gu, J., Liu, Y., Dong, C., Qiao, Y., and Change Loy, C., "ESRGAN: Enhanced super-resolution generative adversarial networks," in [*Proceedings of the European Conference on Computer Vision (ECCV) Workshops*], (September 2018).

[49] Lim, B., Son, S., Kim, H., Nah, S., and Mu Lee, K., "Enhanced deep residual networks for single image super-resolution," in [*Proceedings of the IEEE conference on computer vision and pattern recognition workshops*], 136–144 (2017).

[50] Shi, W., Caballero, J., Huszár, F., Totz, J., Aitken, A. P., Bishop, R., Rueckert, D., and Wang, Z., "Real-time single image and video super-resolution using an efficient sub-pixel convolutional neural network," in [*Proceedings of the IEEE conference on computer vision and pattern recognition*], 1874–1883 (2016).

[51] Ayazoglu, M., "Extremely lightweight quantization robust real-time single-image super resolution for mobile devices," in [*Proceedings of the IEEE/CVF Conference on Computer Vision and Pattern Recognition*], 2472–2479 (2021).

[52] Garrido-Jurado, S., Muñoz-Salinas, R., Madrid-Cuevas, F. J., and Marín-Jiménez, M. J., "Automatic generation and detection of highly reliable fiducial markers under occlusion," *Pattern Recognition* **47**(6), 2280–2292 (2014).